

6.780 – Semiconductor Manufacturing

Term Project – Data Analysis

[Integrated Model-Based Run-to-Run Uniformity Control for Epitaxial Silicon Deposition]

Aaron Elwood Gower-Hall

Roland Sargeant (*LFM '03*), Erik Smith (*LFM '03*)

Abstract— This paper analyzes data taken by Gower-Hall for his MIT PhD thesis. In his thesis, Gower-Hall examines run-to-run control of epitaxial film deposition by way of thickness and resistivity measurements of the film deposited. Our main focus is analysis of the resistivity data captured from the experiments. We give an overview of the thesis, confirm Gower-Hall's findings of the main factors influencing resistivity with basic data analysis, and then extend the analysis of the resistivity measurements.

Index Terms— ANOVA modeling, design of experiments, epitaxial deposition, resistivity, factorial experiment, spatial modeling, spatial thickness, uniformity.

I. INTRODUCTION

Gower-Hall proposes in his thesis a testbed system for integrated model-based, run-to-run control of epitaxial silicon (epi) film deposition, incorporating a cluster tool with a single-wafer epi deposition chamber, an in-line epi film thickness measurement tool, and off-line thickness and measurement systems.[1] He performs a large set of designed experiments to gather information about the system and build process models. The resulting data is analyzed in terms of process stability and noise, process model construction and process optimization. He then presents simulated run-to-run control scenarios using the resulting noise characteristics, time-based models for thickness, and linear models for resistivity.

It is the models for resistivity that this study verifies and improves upon. In accomplishing this aim this paper first gives a description and summary of Gower-Hall's experimental design, results and findings related to resistivity. Next a 'first-level' analysis is performed that duplicates and verifies the original Gower-Hall resistivity findings. This analysis is then improved by incorporating positional information as an explicit parameter in the experimental analysis. These findings are then compared to Gower-Hall's. The paper concludes with a summary of findings and takeaways from this exercise.

II. EXPERIMENT DESIGN

A. Physical Experiment

Epitaxial deposition is a process whereby a thin single crystal film is grown on a single crystal substrate. Chemical

Vapor Deposition (CVD) was performed using an Applied Materials Centura system with an epi deposition chamber as the deposition tool.

The physical and electrical properties of the epitaxial film are important to the functionality of the final device. Physical properties for the epi layer include surface quality, crystallographic defects and film thickness. Important electrical properties include minority carrier lifetimes and *film resistivity*.

Film resistivity ($\Omega\text{-cm}$) is the focus of this paper and is directly related to the concentration of dopant material in the epi layer through the relation

$$\rho = \frac{1}{qn\mu} \quad (\text{Equation. 2-1})$$

where q is the electronic charge (Coulombs), n is the doping concentration (atoms/cm³) and μ is the carrier mobility (cm²/v sec).

The resistivity measurements were taken in four repetitions of a single diameter scan (with 21 sites) as shown in Figure 2-1. The four scans were reviewed and the "best" one selected for each wafer. This best scan was averaged, where there was a single center point and two measurements for all other radii, resulting in 11 radial site resistivities. Only 10 sites were retained for analysis since the outermost resistivity measurements demonstrated high variation that was not well modeled.

B. Design of Experiment (DOE)

Gower-Hall's DOE was composed of 128 two-level fractional factorial design points, 18 axial points, 8 center points, and 4 additional replicates of a randomly chosen fractional design point, for a total of 158 runs¹. There were nine parameters, excluding deposition time, which was held constant across all of the experiments.

A full factorial design with 9 parameters at two levels would

¹ An important note is that the team only had a portion of this data to work with. Specifically, only 112 data groups were provided, one group for each separate treatment or experimental run, with 19 sites per data group.

require 512 experiments, but a 1/4 fractional design was used to select only 128 design points. Table 2-1 below shows the parameters and levels used in the experimental design.

FIGURE 2-1: Resistivity Measurement Map

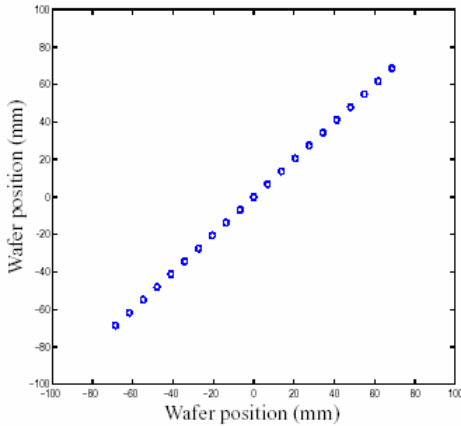


TABLE 2-1: DOE Input Levels

Factor	Lower axial (-α)	Lower (-1)	Center (0)	Upper (+1)	Upper axial (+α)
Deposit time (sec)	N/A	N/A	50	N/A	N/A
Deposit temperature (°C)	1090 (-1.500)	1100	1120	1140	1150 (1.500)
Dopant mixing ratio (%)	20 (-1.500)	30	50	70	80 (1.500)
Dopant main flow (sccm)	40 (-1.571)	80	150	220	260 (1.571)
% Lower power	45 (-1.667)	47	50	53	55 (1.667)
% Inner power	40 (-1.429)	43	50	57	60 (1.429)
Dilutant (H ₂) flow (slm)	30 (-1.500)	35	45	55	60 (1.500)
Trichlorosilane (TCS) flow (slm)	10 (-1.667)	10.8	12	13.2	14 (1.667)
Center gas flow valve (Accusett inner setpoint)	115 (-1.667)	123	135	147	155 (1.667)
Outer gas flow valve (Accusett outer setpoint)	60 (-1.667)	68	80	92	100 (1.667)

C. Experimental Results and Findings

Gower-Hall first shows that there is much more variation in the outputs in terms of mean-shift noise and individual site noise for resistivity than for thickness. (See Table 2-2) The standard deviation of the noise appears to be considerably higher for resistivity than for thickness measurements.

More importantly, Gower-Hall determines that the inputs most significantly affecting resistivity are:

- Dopant Ratio
- H₂ Flow
- TCS Flow
- Deposit Temperature

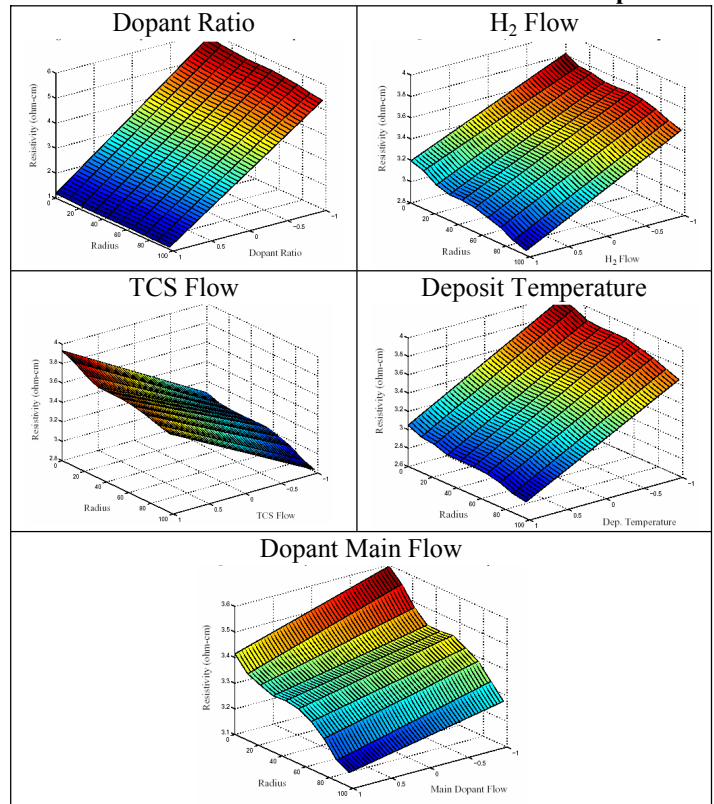
Gower-Hall notes that even though Dopant Main Flow is not a significant effect, since it is known to be a control knob

for fine tuning resistivity, he includes it in his model. He also notes that Dopant Ratio has by far the strongest effect on the outputs, and that all others have significantly weaker effects. Figure 2-2 below plots the modeled resistivity for each radial site as a first-order function of the significant inputs. These plots are taken directly from Gower-Hall’s thesis.

TABLE 2-2: Noise estimates for the DOE Replicates

Replicate Type	Type of Noise	Std. Dev. Of Noise Thickness	Std. Dev. Of Noise Resistivity
Center	Mean shift noise $\hat{\sigma}_{\mu}$	0.46%	2.87%
Center	Site Noise $\hat{\sigma}_{site}$	0.14%	1.34%
Fractional Factorial	Mean shift Noise $\hat{\sigma}_{\mu}$	0.35%	2.57%
Fractional Factorial	Site Noise $\hat{\sigma}_{site}$	0.12%	2.13%

FIGURE 2-2: First-order functions in terms of inputs



Gower-Hall then describes some possible mechanisms why each of these parameters affects the output in the way that they do.

With the unadjusted DOE data, the first order (linear) models capture and average of 91.9% of the variation while the second order polynomials capture approximately 97.6%. He finds that neither first order nor second order models represent the resistivity data as well as the thickness data.

Possible reasons given for this phenomenon are the high measurement and process noise and that the response surface may require a high order model.

Gower-Hall also notes that the models do not demonstrate strong controls for manipulating the resistivity uniformly across the surface of the wafer. That is, the plots demonstrate an ability to shift the resistivity profile up and down but do not indicate that the resistivity near the wafer's center can be adjusted relative to the resistivity near the wafer's edge. Another important observation is that, while the film may be non-uniform in thickness, film thickness has little effect on resistivity. Resistivity can still be relatively uniform even when film thickness varies since film composition is resistivity's most important determinant.

III. VERIFICATION OF GOWER-HALL'S RESULTS

A. Design of Experiment

The method for verifying Gower-Hall's results was similar to that followed by Gower-Hall himself. In brief, the research team used Gower-Hall's data, analyzing the same factors to determine the best model for estimating resistivity. For each experiment treatment, the team "threw away" position data by averaging across all nineteen positions to obtain an average value for that experiment.

Using the JMPIn statistical package, the team ran a Fit Model instruction that determined initial estimates and their significance. Non-significant factors were iteratively removed from the model until only significant factors affecting resistivity remained.

B. Results and Findings

The model obtained does not include Dopant Main Flow as an important figure because it was clearly not significant in the analysis (the resulting t-Ratio for Dopant Main Flow was -0.72 and the Prob >|t| was 0.4732). However, as mentioned previously, Gower-Hall felt inclined to include it in because it is a well-known control knob for fine tuning resistivity.

Apart from this discrepancy, the resulting model from this analysis verified the significance of Deposit Temperature, Dopant Ratio, H₂ Flow and TCS Flow as sensitive main effect inputs to film resistivity. (In this model, these input parameters are respectively termed x_1 , x_2 , x_3 , and x_4). However, the team also determined that there are three significant one-way interactions:

- Deposit Temperature * TCS Flow [x_1*x_4]
- Deposit Temperature * Dopant Mix [x_1*x_2]
- Dopant Mix * H₂ Flow [x_2*x_3]

The model for resistivity is Equation 3-1:

$$y = 3.345 - 0.446x_1 - 2.236x_2 - 0.292x_3 + 0.376x_4 - 0.270x_2x_4 + 0.321x_1x_2 + 0.198x_2x_3$$

Adjusted R-squared for this model is 95.6244%, which should convince the reader of the model's overall efficacy.

A summary of this model's coefficients including relevant statistics that demonstrate each coefficient's significance is provided in Table 3-1.

TABLE 3-1: Preliminary model Estimates

Term	Estimate	Std Error	t Ratio	Prob> t
Intercept	3.34485	0.044178	75.71	< .0001
Dep. Temp (x_1)	-0.4457	0.048131	-9.26	< .0001
Dop. Mix (x_2)	-2.2359	0.048926	-45.7	< .0001
Dil. H ₂ (x_3)	-0.2919	0.048298	-6.04	< .0001
TCS Flow (x_4)	0.37592	0.047820	7.86	< .0001
Dep Temp * Dop Mix	0.32050	0.049333	6.5	< .0001
Dop Mix * Dil H ₂	0.19822	0.049519	4	< .0001
Dop Mix * TCS	-0.27007	0.049299	-5.48	< .0001

It is important to note that the interaction between Outer Gas Flow and Percent Inner Power seemed to be significant but individually, their main effects were not significant. The team believes this to be a limitation of the statistical application (JMP). That is, the package does not allow interaction terms to be included in a model without its corresponding first-level effects also being included. Since this interaction term had a relatively minor effect, and for the sake of simplicity (seven model terms instead of ten terms), the team chose to exclude it from the model.

Figure 3-1 gives the ANOVA summary of the error associated with the model and lack-of-fit.

FIGURE 3-1: ANOVA Summary Statistics

Analysis of Variance				
<u>Source</u>	<u>DF</u>	<u>Sum of Squares</u>	<u>Mean Square</u>	<u>F Ratio</u>
Model	7	528.59914	75.5142	347.5453
Error	104	22.59698	0.2173	Prob > F
C. Total	111	551.19612		< .0001
Lack of Fit				
<u>Source</u>	<u>DF</u>	<u>Sum of Squares</u>	<u>Mean Square</u>	<u>F Ratio</u>
Model	15	9.957507	0.663834	4.6743
Error	89	12.639468	0.142016	Prob > F
C. Total	104	22.596975		< .0001
				Max RSq
				0.9771

The very low probability of Lack of Fit gives further evidence for the model's usefulness in describing the relationship between the control parameters and the underlying data.

The analysis to this point verifies Gower-Hall's results with the noted omission of Dopant Main Flow as a control parameter. In addition, it actually extends Gower-Hall's analysis slightly by explicitly quantifying these effects, which

Gower-Hall does only indirectly by means of the plots displayed in Figure 2-2.

48.67% ($\beta_2\beta_3$, one-way interaction of Dop Mix Ratio and Dil H2 Flow).

IV. SECOND-LEVEL ANALYSIS

A. Design of Experiment

At this point, instead of blindly fitting more models to the data, the team took a step back and simply looked at the raw data in the hopes of gaining further intuition into the underlying dynamics governing resistivity. The result of this was the hypothesis that the resistivity model might have a positional component – specifically, the team surmised that radial distance from the center of the wafer might affect resistivity.

Figure 4-1 below shows a plot of all 112 experiments in the provided data set, with each arrangement of colored connected points representing a different experiment, and each point representing a measurement at the indicated position. In the data provided, each experiment or treatment has a total of 19 separate measurements sites. These sites are located in a line across the wafer diameter with radial distances from -87.3 to $+87.3$ cm in 8.7 cm increments.

A naïve analysis of the data suggests that there might be a positional trend in the data, with the resistivity peaking at the center of the wafer. This observation prompted the team to plot the average resistivity by site. This is shown in Figure 4-2. At first glance, it appears that resistivity may peak in the center of the wafer and that radial displacement from the center of the wafer may affect resistivity.

This led the team to ask the question “If there is some effect due to radial displacement from the center of the wafer, what is that effect?”

B. Results and Findings

The team’s first attempt to investigate positional effects was to perform an analysis, where we built a separate model for each of the nineteen points (in contrast, the model developed before was an aggregate model across the surface of the wafer since it averaged data for each experiment across those nineteen points). See Figure 4-3 below.

This analysis yielded the results summarized in Table 4-1, where each row provides the coefficients for a separate site on the wafer (for instance, the site at -87.3 cm or the site at $+29.1$ cm) for Equation 4-1:

$$y = \beta_1x_1 + \beta_2x_2 + \beta_3x_3 + \beta_{41}x_4 + \beta_{12}x_{12} + \beta_{23}x_{23} + \beta_{24}x_{14}$$

Table 4-1 illustrates that there is a large degree of disparity in the model coefficients for individual sites. In the best case, the minimum amount of difference between the maximum and minimum coefficients between the 19 site models is 9.70% (β_1 , Dep Temp), and in the worst case this difference is

FIGURE 4-1: Plot of Raw data across the Wafer

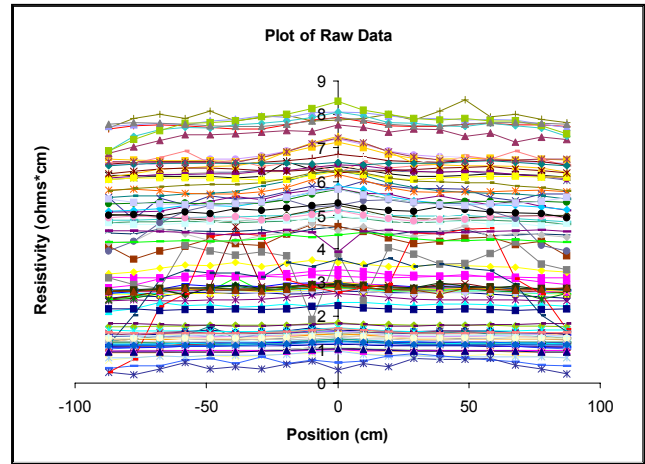


FIGURE 4-2: Plot of Average Resistivity by Position

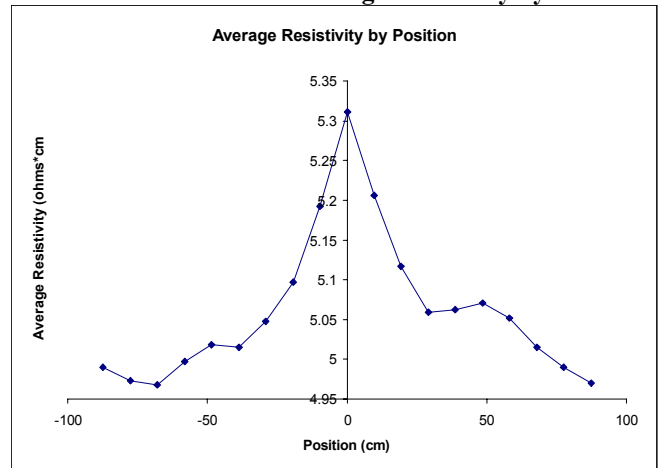


FIGURE 4-3: Individual Model for Nineteen Points

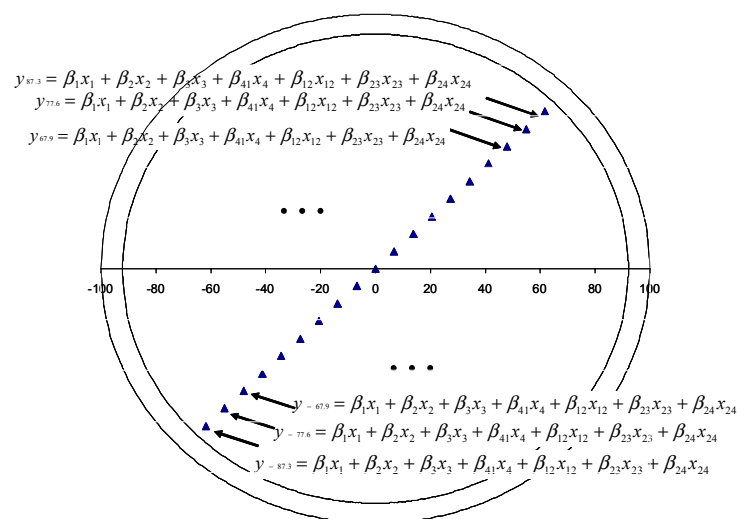


TABLE 4-1: Individual Site Model Parameter Estimates

	Int	β_1	β_2	β_3	β_4	$\beta_1\beta_2$	$\beta_2\beta_3$	$\beta_2\beta_4$	R^2 -adj	Prob LOF
-87.3	3.184	-0.414	-2.117	-0.317	0.388	0.298	0.232	-0.283	0.897	<0.0001
-77.6	3.212	-0.435	-2.138	-0.321	0.383	0.319	0.230	-0.279	0.909	<0.0001
-67.9	3.276	-0.432	-2.192	-0.313	0.369	0.315	0.213	-0.265	0.940	<0.0001
-58.2	3.319	-0.429	-2.216	-0.320	0.357	0.300	0.223	-0.250	0.954	<0.0001
-48.5	3.346	-0.449	-2.244	-0.304	0.348	0.321	0.196	-0.256	0.969	<0.0001
-38.8	3.364	-0.456	-2.249	-0.286	0.348	0.328	0.192	-0.244	0.967	<0.0001
-29.1	3.360	-0.456	-2.256	-0.285	0.355	0.334	0.188	-0.252	0.967	<0.0001
-19.4	3.401	-0.440	-2.282	-0.280	0.389	0.309	0.189	-0.280	0.959	<0.0001
-9.7	3.440	-0.470	-2.280	-0.242	0.424	0.330	0.156	-0.313	0.942	0.0005
0	3.493	-0.450	-2.327	-0.258	0.425	0.327	0.173	-0.311	0.953	<0.0001
9.7	3.441	-0.462	-2.296	-0.252	0.418	0.331	0.166	-0.307	0.948	<0.0001
19.4	3.392	-0.430	-2.276	-0.285	0.380	0.308	0.192	-0.277	0.958	<0.0001
29.1	3.369	-0.448	-2.258	-0.283	0.359	0.325	0.190	-0.256	0.968	<0.0001
38.8	3.374	-0.454	-2.264	-0.281	0.362	0.326	0.182	-0.259	0.968	<0.0001
48.5	3.385	-0.458	-2.269	-0.290	0.358	0.329	0.190	-0.251	0.967	<0.0001
58.2	3.361	-0.455	-2.250	-0.295	0.360	0.328	0.200	-0.247	0.967	<0.0001
67.9	3.329	-0.441	-2.230	-0.312	0.361	0.315	0.214	-0.250	0.956	<0.0001
77.6	3.280	-0.450	-2.190	-0.307	0.378	0.326	0.214	-0.271	0.941	0.0003
87.3	3.227	-0.441	-2.149	-0.316	0.382	0.323	0.226	-0.278	0.924	0.0221
max	3.493	-0.414	-2.117	-0.242	0.425	0.334	0.232	-0.244	0.969	0.0221
min	3.184	-0.470	-2.327	-0.321	0.348	0.298	0.156	-0.313	0.897	0.0003
% diff	9.70%	13.37%	9.89%	32.89%	22.22%	12.13%	48.67%	28.09%		

An interesting result from this analysis is that each one of the site models contains the same four main effects and three one-way interactions previously found to be significant in the previous model, where position data was averaged. In addition, none of these individual site models has any additional terms besides these seven.

Another important observation is that the 19 models, for the most part, do a decent job of describing the influence that the input parameters have on resistivity at each site. Despite this, there is a fair degree of variation in the “goodness” of the models, with the models’ ability to describe the underlying process appearing to fall off towards the edge of the wafer surface. In the most cases, towards the wafer center, R^2 -adj is between 94 and 96%, while towards the edges R^2 -adj appears to fall off, being just just 89.7% at position -87.3cm and 92.4% at +87.3cm. Similarly, most site models have a very low probability of Lack of Fit - <0.0001%. However, some models, including one near the center, have slightly higher probabilities, with the model at position +87.3cm having a 2.21% probability of a Lack of Fit.

Thus, although the 19 models do a decent job of describing what is occurring in regards to resistivity for each site, there is significant variation between each of the models. In addition, this method has two clear disadvantages of practical consequence to the engineer who wishes to understand the underlying behavior in the system. In the first place, it is difficult to keep track of coefficients for all 19 models. When the intercept for each model is included, the engineer must deal with a total of 152 (8*19) model coefficients. A second disadvantage of this method is that it is not clear how to interpolate between the 19 discrete sites.

The team’s second attempt at analyzing the data was fitting a model including position on the wafer as an additional explicit parameter. In effect, the team transposed position data for each experiment into another column in the dataset.

Model coefficients for this analysis, where the team used radial distance from the center of the wafer as the explicit

parameter, are provided in Table 4-2 below. Results for an intermediate analysis in which position was considered as a parameter (as opposed to radial distance) are not discussed.

TABLE 4-2: Parameter Estimates for Full Model Including Radial Position as an Explicit Parameter

Parameter Estimates	Estimate	t Ratio	Prob> t
Intercept	2.797	168.47	0
Center Gas Flow Valve	-0.014	-1.64	0.1006
Outer Gas Flow Valve	0.005	0.56	0.5771
Dep Temp	-0.438	-54.33	0
Dop Mix Ratio	-2.256	-266.9	0
Dop Main Flow	-0.017	-2.03	0.0423
% Lower Power	0.007	0.9	0.3691
% Inner Power	0.034	4.14	<0.0001
Dil H2 Flow (slm)	-0.303	-38.46	<0.0001
TCS flow (slm)	0.363	45.26	0
Radial Xformed	-0.119	-10.1	<0.0001
(Dop Mix Ratio+0.00893)*(Dop Mix Ratio+0.00893)	0.698	37.52	<0.0001
(Center Gas Flow Valve-0.08036)*(Dop Mix Ratio+0.00893)	-0.039	-4.54	<0.0001
(Center Gas Flow Valve-0.08036)*(Dop Main Flow-0.00893)	0.028	3.15	0.0017
(Center Gas Flow Valve-0.08036)*(% Lower Power+0.00893)	-0.037	-4.35	<0.0001
(Center Gas Flow Valve-0.08036)*(% Inner Power+0.02679)	0.022	2.41	0.0161
(Center Gas Flow Valve-0.08036)*(TCS flow (slm)-0.02679)	-0.029	-3.33	0.0009
(Center Gas Flow Valve-0.08036)*(Radial Xformed-0.05263)	-0.035	-2.61	0.0092
(Outer Gas Flow Valve+0.13095)*(Dep Temp-0.02679)	0.068	8.03	<0.0001
(Outer Gas Flow Valve+0.13095)*(Dop Main Flow-0.00893)	-0.065	-7.35	<0.0001
(Outer Gas Flow Valve+0.13095)*(% Inner Power+0.02679)	-0.127	-14.12	<0.0001
(Outer Gas Flow Valve+0.13095)*(Dil H2 Flow (slm)+0.04464)	-0.046	-5.21	<0.0001
(Outer Gas Flow Valve+0.13095)*(TCS flow (slm)-0.02679)	0.076	8.54	<0.0001
(Outer Gas Flow Valve+0.13095)*(Radial Xformed-0.05263)	0.045	3.31	0.001
(Dep Temp-0.02679)*(Dop Mix Ratio+0.00893)	0.310	37.37	<0.0001
(Dep Temp-0.02679)*(Dop Main Flow-0.00893)	0.068	7.97	<0.0001
(Dep Temp-0.02679)*(% Inner Power+0.02679)	0.045	5.33	<0.0001
(Dep Temp-0.02679)*(Dil H2 Flow (slm)+0.04464)	0.118	14.1	<0.0001
(Dep Temp-0.02679)*(TCS flow (slm)-0.02679)	-0.054	-6.52	<0.0001
(Dop Main Flow-0.00893)*(% Inner Power+0.02679)	-0.040	-4.68	<0.0001
(Dop Main Flow-0.00893)*(TCS flow (slm)-0.02679)	0.034	3.85	0.0001
(Dop Mix Ratio+0.00893)*(% Lower Power+0.00893)	0.026	3.14	0.0017
(Dop Mix Ratio+0.00893)*(Dil H2 Flow (slm)+0.04464)	0.171	19.26	<0.0001
(Dop Mix Ratio+0.00893)*(TCS flow (slm)-0.02679)	-0.254	-30.27	<0.0001
(Dop Mix Ratio+0.00893)*(Radial Xformed-0.05263)	0.081	6.18	<0.0001
(% Lower Power+0.00893)*(Dil H2 Flow (slm)+0.04464)	-0.079	-9.16	<0.0001
(% Lower Power+0.00893)*(TCS flow (slm)-0.02679)	0.050	6.02	<0.0001
(% Inner Power+0.02679)*(TCS flow (slm)-0.02679)	0.023	2.78	0.0055
(Dil H2 Flow (slm)+0.04464)*(Radial Xformed-0.05263)	-0.031	-2.42	0.0155
(% Inner Power+0.02679)*(Radial Xformed-0.05263)	0.048	3.78	0.0002

FIGURE 4-3: Full Model ANOVA Summary Statistics – Radial Distance Included as an Explicit Parameter

Summary of Fit				
RSquare	0.978321			
RSquare Adj	0.977916			
Root Mean Square Error	0.331037			
Mean of Response	3.392218			
Observations (or Sum Wgts)	2128			
Analysis of Variance				
Source	DF	Sum of Squares	Mean Square	
Model	39	10325.661	264.761	
Error	2088	228.815	0.11	
C. Total	2127	10554.476		
Lack Of Fit				
Source	DF	Sum of Squares	Mean Square	F Ratio
Lack Of Fit	1000	216.53874	0.216539	17.2471
Pure Error	1088	12.27616	0.011283	Prob > F
Total Error	2088	228.81491		<0.0001
Max RSq				0.9999

As Table 4-2 demonstrates, 36 main effects and one-way interactions were significant to at least 95%, with 25 of these

terms being significant to $<0.0001\%$. An interesting observation is that, although the main effects of Center Gas Flow, Outer Gas Flow, and % Lower Power are not significant, several of their interaction terms are. The full model performs very well with an R^2 -adj of 97.8% and probability of a Lack of Fit of $<0.0001\%$. Summary statistics for the model are shown in Figure 4-3.

Although this model demonstrates that many more parameters affect the final parameter of interest – resistivity – it is likely that an engineer would find it of little practical use since it has so many terms. The exception to this, however, might be if that engineer could develop an automated system that could use the full model to control a process.

With this in mind, the research team pared the model down to include just eight terms - the seven significant terms from the previous analyses and radial distance. The results for this model (Table 4-2 and Figure 4-4) illustrate that even with just these eight terms, little resolution is lost in explaining the underlying variation; R^2 -adj is still a respectable 95.2%, and probability of a Lack of Fit is still $<0.0001\%$.

TABLE 4-2: Parameter Estimates for Simplified Model Including Radial Distance

Term	Estimate	Std Error	T Ratio	Prob> t
Intercept	3.3511	0.0106	316.15	0.0000
Dep Temp	-0.4457	0.011506	-38.74	$<.0001$
Dop Mix Ratio	-2.2360	0.011696	-191.2	0.0000
Dil H2 Flow (slm)	-0.2919	0.011546	-25.28	$<.0001$
TCS flow (slm)	0.3759	0.011432	32.88	$<.0001$
(Dep Temp-0.02679)*(Dop Mix Ratio+0.00893)	0.3205	0.011793	27.18	$<.0001$
(Dop Mix Ratio+0.00893)*(Dil H2 Flow (slm)+0.04464)	0.1982	0.011838	16.74	$<.0001$
(Dop Mix Ratio+0.00893)*(TCS flow (slm)-0.02679)	-0.2701	0.011785	-22.92	$<.0001$
Radial Xformed	-0.1186	0.01723	-6.88	$<.0001$

V. CONCLUSION

In this paper, we verified the findings of Gower-Hall with regards to the significant parameters affecting resistivity. Furthermore we determined that position, though being significant in the model, contributes some variation to resistivity.

Currently, the pattern map used by Gower-Hall to measure resistivity is a one-dimensional line of points across the wafer diameter. An improved map would be any kind of two-dimensional pattern, such as the pattern used for thickness. This method would provide a better estimate of the effect of

resistivity variance as a function of radial displacement from the wafer center. This would also facilitate analysis of resistivity nonuniformity across the face of the wafer.

FIGURE 4-4: ANOVA Summary Statistics for Simplified Model Including Radial Distance

Summary of Fit

RSquare	0.952635
RSquare Adj	0.952456
Root Mean Square Error	0.485717
Mean of Response	3.392218
Observations (or Sum Wgts)	2128

Analysis of Variance

Source	DF	Sum of Squares	Mean Square
Model	8	10054.559	1256.82
Error	2119	499.918	0.24
C. Total	2127	10554.476	

Lack Of Fit

Source	DF	Sum of Squares	Mean Square	F Ratio
Lack Of Fit	221	203.0612	0.918829	5.8747
Pure Error	1898	296.85636	0.156405	<0.0001
Total Error	2119	499.91756		
				Max RSq 0.9719

Areas that merit further research include the following:

It would have been useful to have data for all 158 experimental runs. The team probably lost some resolution in the analysis as a result of the lack of this data.

In the data provided, deposition time was kept constant at 50 sec. As a result, it is not clear what effect time might have on resistivity. Further experimentation might help establish what, if any, relationship might be present.

The research team accepted Gower-Hall's assumption that thickness and resistivity are not correlated. Despite this, the team feels that this relationship, or lack thereof, warrants further investigation.

REFERENCES

- [1] A. E. Gower-Hall, "Integrated Model-Based Run-to-Run Uniformity Control for Epitaxial Silicon Deposition," MIT Thesis, 2001

Roland Sargeant (BS'97-SM'03 – MBA '03) hereafter referred to as Sarge. Sarge likes to hang out on the beach in Barbados with his plastic arm floaties (he can't swim).

Erik Smith (BS'94-SM'03-MBA'03) hereafter referred to as Skipper. Skipper can swear like a sailor.